MATEC Web of Conferences **21**, 04005 (2015)
DOI: 10.1051/matecconf/20152104005

A 3-D analysis of the sheared cross-section of electrical steel plates

Heng-Sheng Lin[1,a], Yu-Da Liu[2], Hsin-Te Wang[2], Kun-Min Huang[2], and Zhe-An Lin[1]

[1] Department of Mold and Die Engineering, National Kaohsiung University of Applied Sciences, Kaohsiung 807, Taiwan, R.O.C.
[2] Metal Industries Research & Development Centre, Kaohsiung 811, Taiwan, R.O.C.

Abstract. Most rotators and stators of motors or generators as well as the cores of transformers are produced by laminated plates of electric steel to reduce the energy loss caused by eddy current. Therefore, it is essential to predict as well as improve the shearing quality of the electric steel plates and thus help increase the efficiency of the machines. Most investigations overlook the planar anisotropy in the numerical analysis of the shearing process. The simplified 2-D analysis was adopted instead of the 3-D analysis. In this work, DEFORM 3D analysis is used which takes into account the anisotropy of the plate material. Normalized Cockcroft & Latham damage criterion is used in determining the occurrence of fracture during the shearing. The result shows that the 3-D analysis predicts well in the burnish depth while roughly in rollover due to insufficient resolution of the element size. The 2-D analysis tends to underestimate the burnish depth attributed to the improper selection of lower critical damage values and predicts scattered rollover.

1. Introduction

Most rotators and stators of motors or generators as well as the cores of transformers are produced by laminated plates of electric steel to reduce the energy loss caused by the eddy current. During the stamping of electric steel plates, distortion of the sheared edge and deterioration of magnetic properties occur attributed to selecting improper punch/die clearance or blank-holder force. Excessive burr height also causes problems in stacking the electric steel plates and consequently producing additional iron loss [1–3]. Therefore, it is essential to predict as well as improve the shearing quality of the electric steel plates and thus help increase the efficiency of motors, generators and transformers.

A survey of literature indicates that most investigations overlook the planar anisotropy in the numerical analysis of the shearing process. The simplified 2-D plane strain or axi-symmetric analysis was adopted instead of the 3-D analysis [4–10]. The advantages with 2-D simulation are the efficiency in computation and the clarity in determining the composition of the sheared cross-section which includes the rollover, burnish, fracture and burr.

[a] Corresponding author: `hslin@kuas.edu.tw`

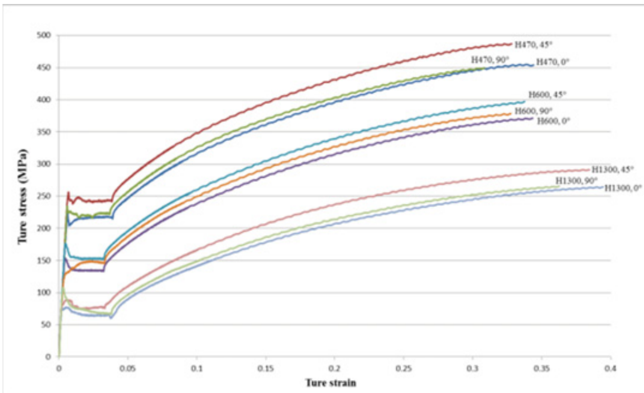

Figure 1. Flow stresses of plate materials.

Table 1. Mechanical properties and critical damage values of plate.

	YS (MPa)	TS (MPa)	R_0	R_{45}	R_{90}	C
H470	314	461	1.044	0.58	1.074	0.545
H600	294	441	1.007	0.879	1.221	0.619
H1300	275	373	1.126	0.645	1.059	0.680

In this work, the 3-D analysis is used which takes into account the anisotropy of the plate materials. Normalized Cockcroft & Latham damage criterion is used in the simulation. Three electrical steel plates are used in analysing the effect of the punch/die clearance and blank-holder force on the composition of the sheared cross-section. The result of the 3-D analysis is compared to that of the 2-D analysis and experiment.

2. Methods

2.1 The materials

Three electrical steel plate materials, H470, H600 and H1300, were used in the investigation, where the numbers correspond to the maximum iron loss (unit 10^{-2} W/kg) of the respective plate materials. Therefore, the lower value is in the iron loss, the higher percentage of additives of silicon and/or aluminium is in the electrical steel plate, as well as a higher strength and lower ductility is with the plate material. The thickness gauge is 0.5 mm. Figure 1 shows the flow stress along the 0, 45 and 90 degrees of rolling orientation of the three electrical steel plates. The mechanical properties and strain ratios (Lankford coefficients) of R_0, $R_4$5 and $R_9$0 are shown in Table 1.

2.2 The shearing experiment

The assembly of punch and die of the shearing experiment is shown in Fig. 2. The blank-folder is removed in the picture for clarity. The die-set is mounted on a mechanical press which operates at a speed ranging from 250 to 510 SPM. The dimension of the shearing and the design parameters are shown in Table 2.

Figure 2. Assembly of punch and die of shearing experiment.

Table 2. Dimensions and parameters used in shearing experiment.

Size of shearing (mm × mm)	150 × 30
Thickness, t (mm)	0.5
Stamping speed (SPM)	250, 380, 510
Punch/die clearance (mm)	0.01 (2% t), 0.0175 (3.5% t), 0.025 (5% t)
Blank-holder force (kN)	6.2, 18.7, 31.1

2.3 The shearing simulation

Commercial finite element software DEFORM 2D and 3D were used in the simulation. Normalized Cockcroft & Latham damage criterion was used in determining the occurrence of fracture during the shearing, which is defined as

$$C = \int_0^{\bar{\varepsilon}_f} \frac{\sigma^*}{\bar{\sigma}} d\bar{\varepsilon} \tag{1}$$

where C is the critical damage value, σ^* is the maximum tensile stress, $\bar{\sigma}$ is the effective stress, $\bar{\varepsilon}$ is the effective strain and $\bar{\varepsilon}_f$ is the critical effective strain upon the fracture of material. The respective critical damage values of the three electrical steel plates are listed in Table 1. They were obtained by matching the damage value of the 3-D simulation with the tensile test upon necking in the width of the tensile specimens. The critical damage value is the greatest with H1300 because its additive is the lowest and toughness is the highest.

Figure 3 shows the modelling for the 3-D simulation. Some simplifications in the workpiece geometry were necessary in obtaining a successful 3-D simulation. The width of the workpiece was reduced to 2 mm and a plane of symmetry was assigned in order to reduce the elements. Only the portion in contact with the blank-holder was used in the modelling. The workpiece was assumed plastic and the punch and die were rigid. There were 150,000 elements used in the 3-D simulation and 13,000 elements used in the 2-D simulation. The friction factor was 0.12 and the shearing speed was assumed to be 1 mm/s. The effect of strain rate and temperature rise was neglected.

3. Results and discussion

Figure 4 shows a typical cross-section of the shearing experiment. The plate material is H470. The punch/die clearance is 0.0175 mm (3.5% t) and the blank-holder force is 6.2 kN. The influence of stamping speed on shearing quality was found to be insignificant in the shearing experiment. Figure 5 shows the iso-view of the corresponding cross-section of shearing obtained from the 3-D simulation. Figures 6 and 7 show the side-views of the cross-section obtained from the 3-D and 2-D simulation, respectively. Both figures show that it is difficult to identify the transition from burnish to fracture from

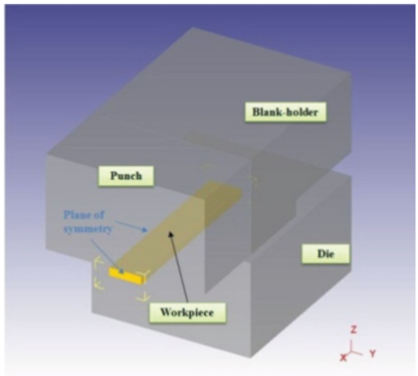

Figure 3. Modelling of 3-D simulation.

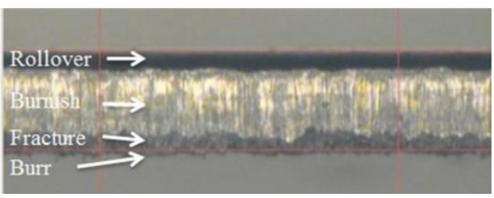

Figure 4. Cross-section of shearing experiment.

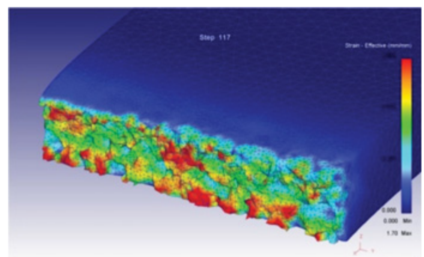

Figure 5. Iso-view of 3-D simulation.

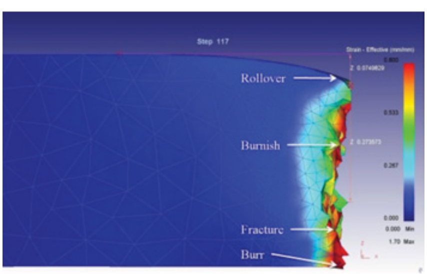

Figure 6. Side-view of 3-D simulation.

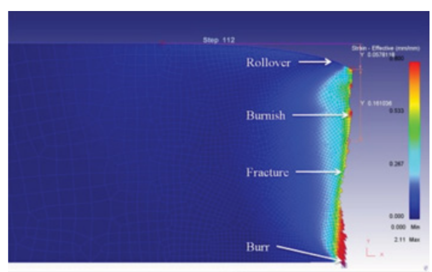

Figure 7. Side-view of 2-D simulation.

the nodal display. Therefore, the load-stroke diagram was also used to help evaluate objectively where the fracture starts, as shown in Fig. 8.

Figure 9 shows that burnish depth decreases as the punch/die clearance increases both in the experiment and simulation. Burnish depth is the largest with plate material H1300 attributed to its highest ductility and hence highest critical damage value. Burnish depth with H600 is in the middle and followed by that of H470. The result of the 3-D simulation agrees well with the experiment while that of the 2-D simulation produces much smaller values and decreases slightly with clearance. Figure 10 shows that burnish depth increases as the blank-holder force increases both in the experiment and simulation. The results with 2-D simulation also produce much smaller values and increase slightly with the BHF.

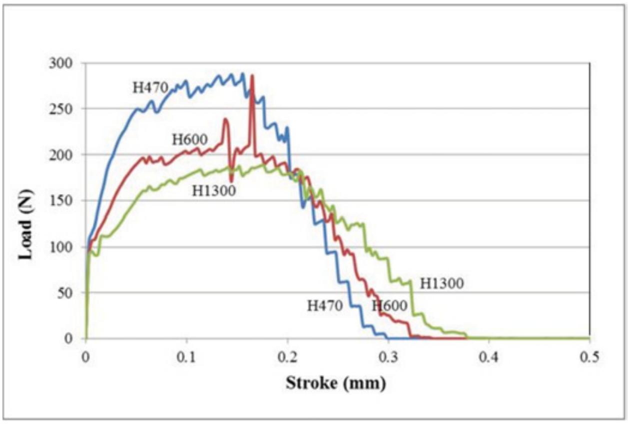

Figure 8. Load-stroke diagram of shearing process.

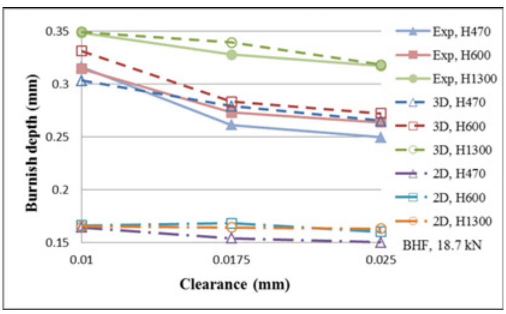

Figure 9. Variation of burnish with clearance.

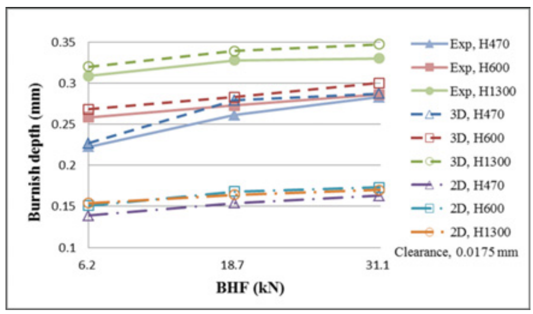

Figure 10. Variation of burnish with BHF.

Both Figs. 9 and 10 indicate that the 2-D simulation tends to underestimate burnish depth and appears insensitive with the variation of punch/die clearance and blank-holder force. The explanation to this discrepancy is improper selection of the critical damage values. They were obtained by matching the tensile test upon necking in the width direction by the 3-D simulation. The same critical damage values were provisionally used in the 2-D simulation. However, these critical damage values were much smaller than the appropriate damage values in the 2-D (plane strain) mode. Higher damage values are expected in the 2-D mode because the necking in the thickness is more difficult to occur than the necking in the width in the 3-D mode. Therefore, the current 2-D simulation predicted early fracture and produced smaller burnish depth because smaller critical damage values were used in the 2-D simulation.

The result of rollover shows that it increases with clearance and decreases with the BHF, as shown in Figs. 11 and 12. However, the 3-D simulation does not predict well in rollover because of insufficient resolution of the element size. The depth of rollover is quite small, which ranges from 0.068 to 0.092 mm, and the element size is about 0.01 mm, as shown in Fig. 6. The adoption or omission of one node at the transition between rollover and burnish can lead to significant discrepancy in judging the depth of rollover. Neither the 2-D simulation predicts well in the rollover. It produces more scattered values as compared to the experiment. Moreover, both experiment and simulation indicate that for a same clearance or BHF, the rollover is the largest with H1300, because of the highest ductility, and followed by those of H600 and H470.

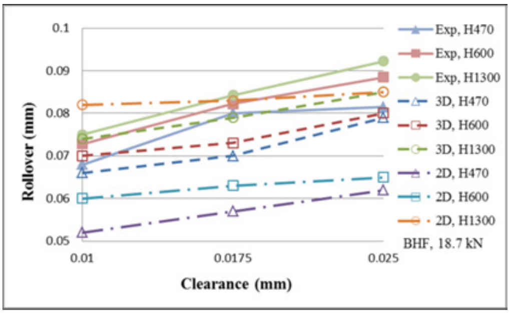

Figure 11. Variation of rollover with clearance.

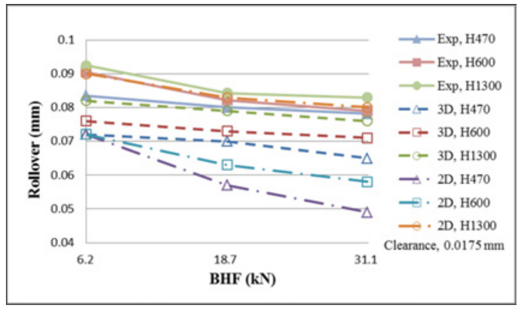

Figure 12. Variation of rollover with BHF.

4. Conclusions

Both the experiment and simulation show that burnish depth decreases with the punch/die clearance and increases with the blank-holder force (BHF). Burnish depth is the largest with plate material H1300 and followed by those of H600 and H470. The result of the 3-D simulation agrees well with the experiment while that of the 2-D simulation tends to underestimate the burnish depth attributed to the improper selection of lower critical damage values.

Rollover increases with clearance and decreases with the BHF. Rollover is the largest with plate material H1300 and followed by those of H600 and H470. However, the 3-D simulation does not predict well in rollover because of insufficient resolution of the element size. The 2-D simulation predicts more scattered values as compared to the experiment.

This work is partly sponsored by the program for graduated scholarship granted by the Metal Industries Research & Development Centre.

References

[1] H. Marouani, A. Ben Ismail, E. Hug, M. Rachik, Mater. Des. **30**, 3566–3571 (2009)
[2] K. Fujisaki, S. Satoh, IEEE Trans. Magn. **40**, 4 (2004)
[3] K. Fujisaki, R. Hirayama, T. Kawachi, S. Satou, C. Kaidou, M. Yabumoto, T. Kubota, IEEE Trans. Magn. **43**, 5 (2007)
[4] D. Brokken, W.A.M. Brekelmans, F.P.T. Baaijens, J. Mater. Process. Technol. **83**, 192–199 (1998)
[5] D. Brokken, W.A.M. Brekelmans, F.P.T. Baaijens, J. Mater. Process. Technol. **103**, 51–56 (2000)
[6] A.M. Goijaerts, L.E. Govaert, F.P.T. Baaijens, J. Mater. Process. Technol. **110**, 312–323 (2001)
[7] S.K. Maiti, A.A. Ambekar, U.P. Singh, P.P. Date, K. Narasimhan, J. Mater. Process. Technol. **102**, 249-256 (2000)
[8] K.H. Shim, S.K. Lee, B.S. Kang, S.M. Hwang, J. Mater. Process. Technol. **155–156**, 1935–1942 (2004)
[9] C. Husson, J.P.M. Correia, L. Daridon, S. Ahzi, J. Mater. Process. Technol. **199**, 74–83 (2008)
[10] B.A. Behrens, A. Bouguecha, M. Vucetic, R. Krimm, T. Hasselbusch, C. Bonk, Procedia Eng. **81**, 1096–1101 (2014)